Integrated Transcriptome and Metabolome Analysis Uncovers Dynamic Regulatory Mechanisms Underlying Inflorescence Development in Agropyron cristatum

Yalin Yu
Chinese Academy of Agricultural Sciences
Xiaojing Qiang
Chinese Academy of Agricultural Sciences
Fan Huang
Chinese Academy of Agricultural Sciences
Yuanfa Meng
Chinese Academy of Agricultural Sciences
Zhiyong Li
Chinese Academy of Agricultural Sciences
Lei Liu
liu43117550@163.com

Chinese Academy of Agricultural Sciences

Article

Keywords: Agropyron cristatum, inflorescence development, transcriptome, phytohormone, gibberellin, auxin, cytokinin, transcription factor, RNA-seq

Posted Date: March 19th, 2026

DOI: https://doi.org/10.21203/rs.3.rs-8960615/v1

Additional Declarations: No competing interests reported.

Integrated Transcriptome and Metabolome Analysis Uncovers Dynamic Regulatory Mechanisms Underlying Inflorescence Development in *Agropyron cristatum*

Yalin Yu[1], Xiaojing Qiang[2], Fan Huang[3], Yuanfa Meng[4], Zhiyong Li[5], and Lei Liu[6*]

[1]Institute of Grassland Research, Chinese Academy of Agricultural Sciences, Hohhot 100081, China
[2]Affiliation, department, city, postcode, country
[*]Correspondence: liu4311755@163.com

ABSTRACT

Agropyron cristatum, a high-quality forage grass and a close relative of wheat (Triticum aestivum), exhibits an inflorescence development process critical for its seed yield and genetic improvement. However, the underlying molecular and hormonal regulatory networks remain poorly understood. In this study, we performed integrated tran-scriptomic sequencing (RNA-seq) and targeted phytohormone profiling on inflores-cences at three developmental stages (booting, heading, and flowering) in A. cristatum. Our metabolomic data revealed dynamic changes in gibberellin (GA), auxin (IAA), and cytokinin (CK) levels, highlighting their pivotal roles during inflorescence develop-ment. Transcriptomic analysis further identified key biosynthesis genes for these hor-mones, including CPS, KAO, KS, GA13ox, GA3ox, GA2ox, TDC, AO1, ALDH, YUCCA, amid, TAA1, miaA, and IPT. In addition, we detected differential expression of critical signaling components, such as GID1 and DELLA, AUX1/LAX, TIR1, ARF, GH3, and SAUR, and CRE1 and B-ARR. We also identified several key transcription factor fami-lies linked to flowering and meristem regulation, including AP2/ERF-ERF, MYB, TCP, HD-ZIP, WOX, LFY, and NF-YC. The current study provides a preliminary elucidation of the hormonal regulatory framework underlying inflorescence development in the *Agropyron cristatum* species complex, offering molecular insights into its inflorescence morphogenesis.

Keywords：Agropyron cristatum; inflorescence development; transcriptome; phytohormone; gibberellin; auxin; cytokinin; transcription factor; RNA-seq

Introduction

Agropyron cristatum, a perennial, densely tufted, high-quality forage grass within the family Poaceae, is renowned for its exceptional cold tolerance, drought resistance, and ability to thrive in poor soils. It exhibits broad ecological adaptability and is dis-tributed across regions including the Middle East, Central Europe, and Central Asia [1]. As a wild relative of wheat, it possesses high nutritional value, an extended green pe-riod, and good palatability, harboring valuable genetic and allelic variation resources for wheat improvement [1-9]. It stands as one of the most important forage grasses in temperate regions [10, 11]. However, inflorescence development, a core agronomic trait determining both its seed yield and forage quality, remains poorly understood at the molecular regulatory level. This knowledge gap severely constrains the progress in breeding for high yield and superior quality, as well as in the innovation of its germplasm resources. Inflorescence architecture is a pivotal agronomic trait determining seed yield, with key parameters such as inflorescence length, spatial distribution of spikelets, and degree of floret differentiation directly influencing final yield components. Studies have shown a positive correlation between inflorescence length and seed yield. Longer inflorescences typically possess greater spikelet-bearing capacity and a more efficient vascular transport system, which facilitates optimized allocation of photoassimilates, thereby enhancing seed-setting rate and grain plumpness [12-14]. However, during in-florescence development, a proportion of florets may abort due to nutrient competition, hormonal imbalance, or pollination constraints, resulting in a lower number of fertile florets compared to the number of morphologically differentiated florets. This consti-tutes a key bottleneck limiting the increase in grains per spike. Therefore, systemati-cally elucidating the regulatory mechanisms underlying inflorescence development in *Agropyron cristatum* is crucial for clarifying the basis of its yield formation and ad-vancing high-yield breeding.

Numerous studies have demonstrated that phytohormones play a central regula-tory role in inflorescence establishment and floret development in grasses. The gradi-ent distribution and signaling of key hormones, including gibberellin (GA), auxin

(IAA), and cytokinin (CK), are indispensable for balancing meristematic activity, maintaining cell determinacy, and regulating the growth of floral organs [15]. In plants, auxin is biosynthesized from tryptophan (TRP) via either the tryptamine (TRA) pathway or alternative, non-TRA pathways [16-19]. During the spikelet initiation stage in barley, enhanced TRA pathway activity establishes a basipetal auxin concen-tration gradient along the developing spike. This gradient influences lateral spikelet development, thereby increasing both the number and density of spikelets per spike [20, 21]. Gibberellin signaling affects inflorescence meristem size and floral patterning primarily by mediating the degradation of DELLA proteins, thereby relieving their re-pressive effects [22]. In rice, the cytokinin oxidase gene OsCKX2 irreversibly degrades CK. The loss-of-function mutant gn1a exhibits significant accumulation of CK in the meristem, leading to a marked increase in branch number and grainnumber per pani-cle [23]. Elevated cytokinin levels can enhance grain number and ultimately boost yield [24, 25]. In summary,multiple phytohormones coordinately regulate the estab-lishment of meristems and floret fertility in wheat and other cereal crops through their intricate networks of biosynthesis, metabolism, and signal transduction.

In recent years, the rapid advancement of high-throughput sequencing technolo-gies has established omics approaches as powerful tools for dissecting the molecular mechanisms underlying inflorescence development. For instance, Hong et al. employed time-series transcriptome analysis to elucidate the regulatory network of flowering in Chinese cabbage [26]. Similarly, Weng conducted a comparative transcriptomic and DNA methylome analysis between two inflorescence types of Panicum hallii, revealing that cytokinin signaling pathways play a crucial role in the divergence of inflorescence architecture and seed size. [27]. Building upon these foundational studies, the present work investigates the dynamic gene expression profiles and phytohormone accumula-tion across three key developmental stages of inflorescence in *Agropyron cristatum*. This integrated analysis provides a robust theoretical framework to support molecular breeding strategies aimed at improving yield-related traits in this important forage grass. .

Results

- Transcriptome Analysis

To explore the dynamic gene expression patterns underlying inflorescence development, we conducted transcriptomic sequencing on inflorescence tissues of *Agropyron cristatum* across three key developmental stages (Figure 1a) : the booting stage (BS), heading stage (HS), and flowering stage (FS). High-throughput sequencing generated high-quality data for all three stages, with each sample yielding at least 6 Gb of clean data and a Q30 base percentage of 95% or higher. Principal component analysis (PCA) of FPKM values revealed clear separation among samples, with distinct clustering within groups in the two-dimensional space (Figure 1a). Pearson correlation analysis indicated high reproducibility across biological replicates, with all pairwise comparisons demonstrating strong consistency (Figure 1b). The analysis results showed that in the comparisons of HS_vs_BS, FS_vs_HS, and FS_vs_BS, there were 5,948, 13,145, and 13,040 significantly upregulated differentially expressed genes (DEGs), and 1,769, 8,342, and 5,637 significantly downregulated DEGs, respectively (Figure 1c). The FS_vs_HS comparison exhibited the most pronounced transcriptomic changes. These transcriptomic findings delineate the stage-dependent dynamics of gene expression during inflorescence development in *A. cristatum.*

(**a**)

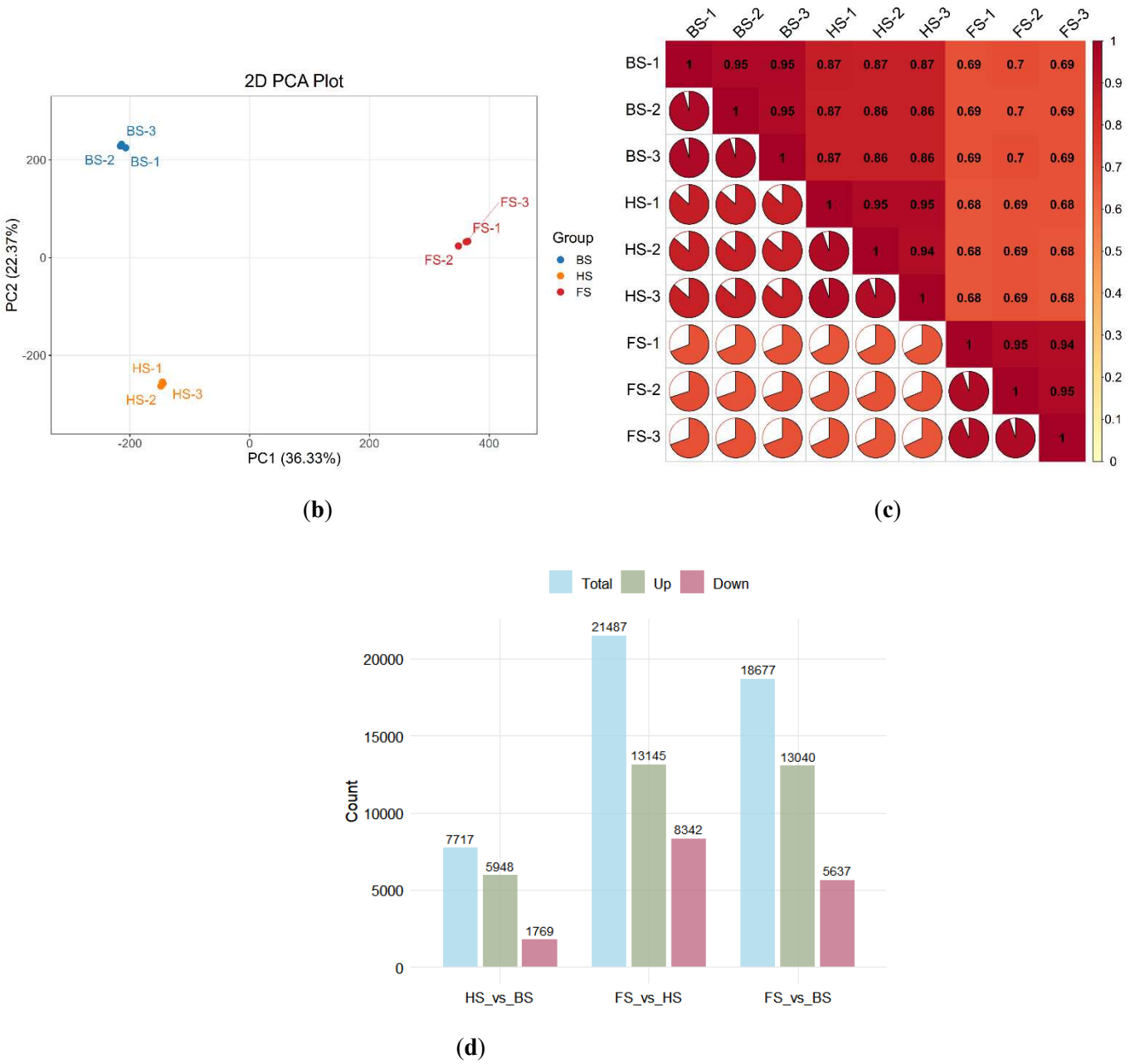

Figure 1. (**a**) Inflorescence morphology of *Agropyron cristatum* at the booting (BS), heading (HS), and flowering (FS) stages. (**b**) Principal component analysis of transcriptomic data across three inflorescence developmental stages in *Agropyron cristatum*. (**c**) Pearson correlation coefficients of gene expression among samples at different inflorescence developmental stages in Agropyron cristatum. (**d**) Statistics of differentially expressed gene numbers across successive inflorescence developmental stages in *Agropyron cristatum*.

- GO and KEGG Enrichment Analyses

Functional annotation of the identified differentially expressed genes (DEGs) was performed using Gene Ontology (GO) classification and Kyoto Encyclopedia of Genes and Genomes (KEGG) pathway enrichment analyses. GO analysis categorized the DEGs into three major classes: biological process (BP), cellular component (CC), and molecular function (MF) (Figure 2). Within the BP category, DEGs were primarily enriched in terms related to cellular process, metabolic process, response to stimulus, biological regulation, and regulation of biological process. In the CC category, DEGs were mainly associated with cellular anatomical entities. Under the MF category, significant enrichment was observed for binding and catalytic activity. KEGG pathway analysis revealed that DEGs were significantly enriched in several key pathways, including Metabolic pathways, Biosynthesis of secondary metabolites, Phenylpropanoid biosynthesis, Galactose metabolism, Cutin, suberine and wax

biosynthesis, and Plant hormone signal transduction. These results suggest that these pathways likely play important roles in inflorescence development.

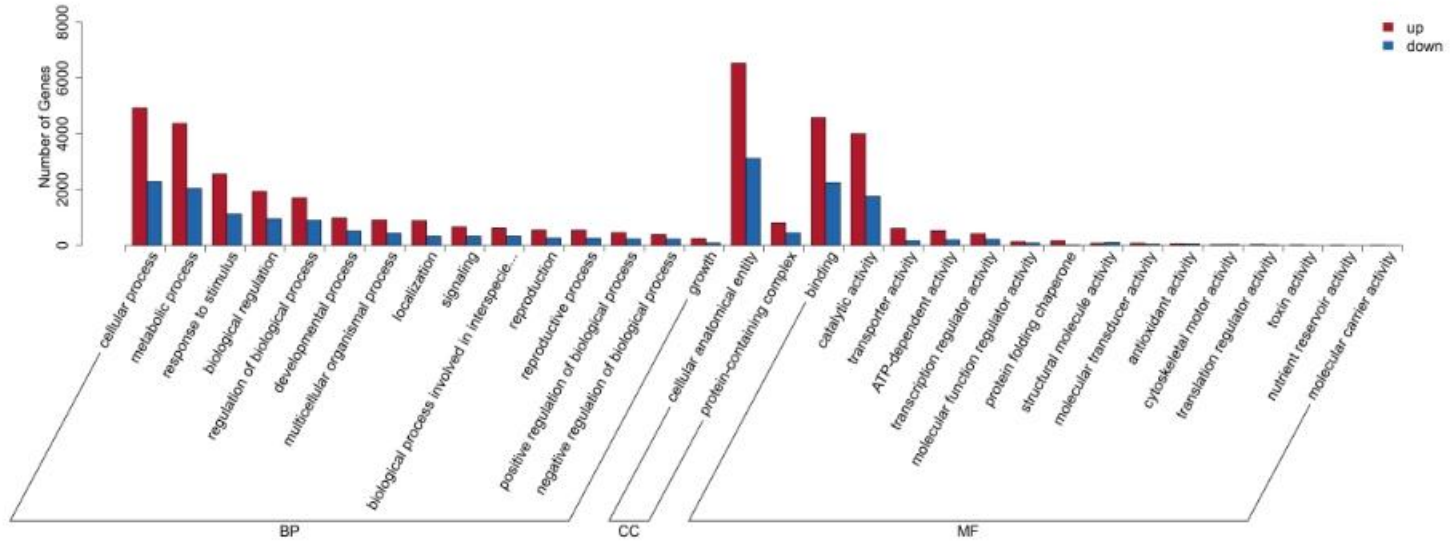

(**a**)

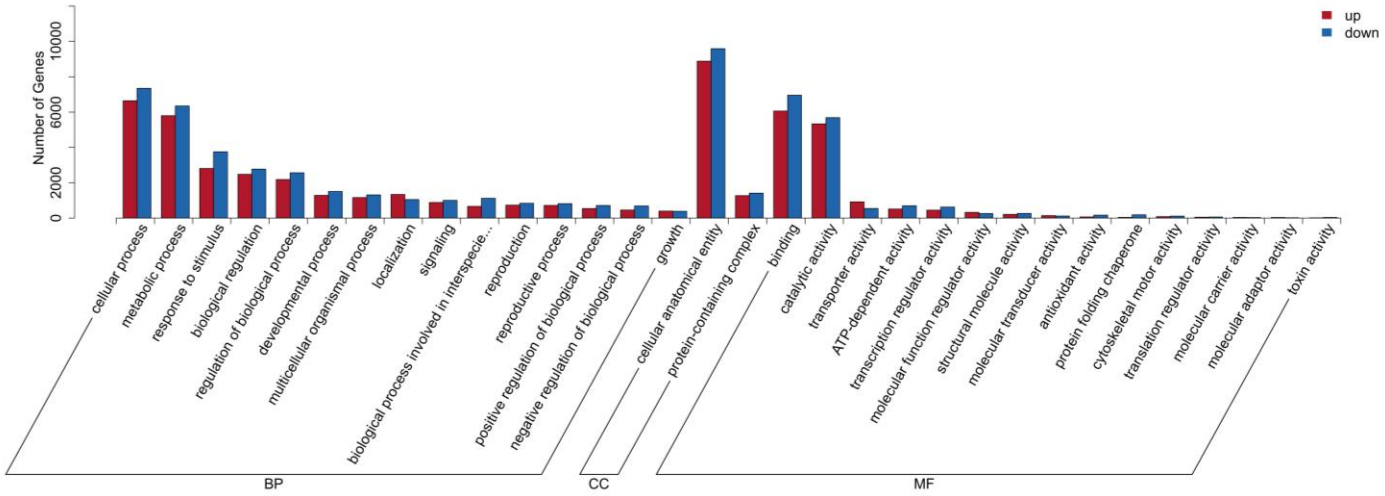

(**b**)

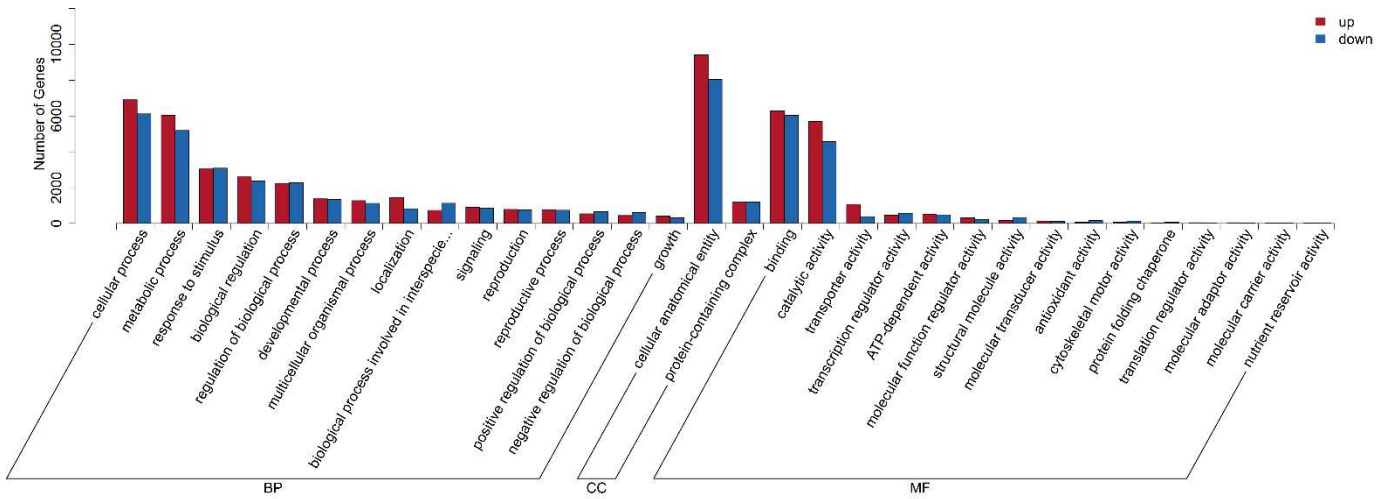
up
down
Number of Genes
0
2000
6000
10000
cellular process
metabolic process
response to stimulus
biological regulation
regulation of biological process
developmental process
multicellular organismal process
localization
biological process involved in interspecie...
signaling
reproduction
reproductive process
positive regulation of biological process
negative regulation of biological process
growth
cellular anatomical entity
protein-containing complex
binding
catalytic activity
transporter activity
transcription regulator activity
ATP-dependent activity
molecular function regulator activity
structural molecule activity
molecular transducer activity
antioxidant activity
cytoskeletal motor activity
protein folding chaperone
translation regulator activity
molecular adaptor activity
molecular carrier activity
nutrient reservoir activity
BP
CC
MF

(**c**)

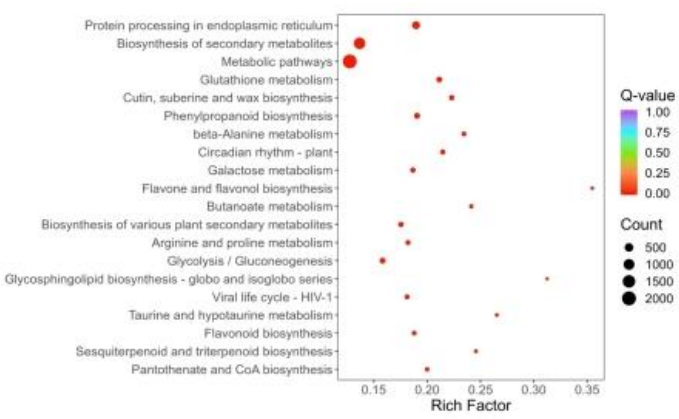
Protein processing in endoplasmic reticulum
Biosynthesis of secondary metabolites
Metabolic pathways
Glutathione metabolism
Cutin, suberine and wax biosynthesis
Phenylpropanoid biosynthesis
beta-Alanine metabolism
Circadian rhythm - plant
Galactose metabolism
Flavone and flavonol biosynthesis
Butanoate metabolism
Biosynthesis of various plant secondary metabolites
Arginine and proline metabolism
Glycolysis / Gluconeogenesis
Glycosphingolipid biosynthesis - globo and isoglobo series
Viral life cycle - HIV-1
Taurine and hypotaurine metabolism
Flavonoid biosynthesis
Sesquiterpenoid and triterpenoid biosynthesis
Pantothenate and CoA biosynthesis
0.15
0.20
0.25
0.30
0.35
Rich Factor
Q-value
1.00
0.75
0.50
0.25
0.00
Count
500
1000
1500
2000

(**d**)

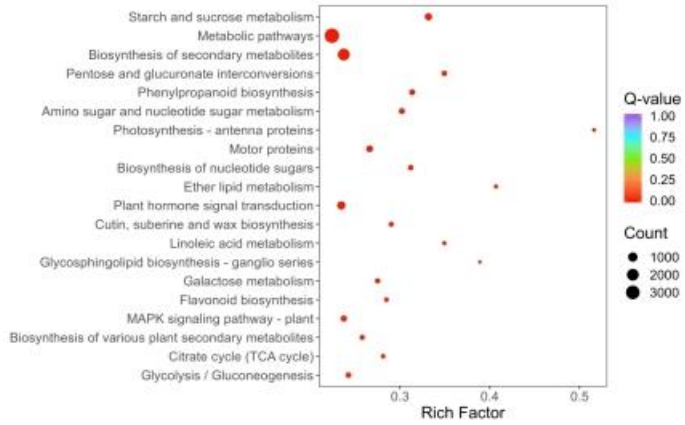
Starch and sucrose metabolism
Metabolic pathways
Biosynthesis of secondary metabolites
Pentose and glucuronate interconversions
Phenylpropanoid biosynthesis
Amino sugar and nucleotide sugar metabolism
Photosynthesis - antenna proteins
Motor proteins
Biosynthesis of nucleotide sugars
Ether lipid metabolism
Plant hormone signal transduction
Cutin, suberine and wax biosynthesis
Linoleic acid metabolism
Glycosphingolipid biosynthesis - ganglio series
Galactose metabolism
Flavonoid biosynthesis
MAPK signaling pathway - plant
Biosynthesis of various plant secondary metabolites
Citrate cycle (TCA cycle)
Glycolysis / Gluconeogenesis
0.3
0.4
0.5
Rich Factor
Q-value
1.00
0.75
0.50
0.25
0.00
Count
1000
2000
3000

(**e**)

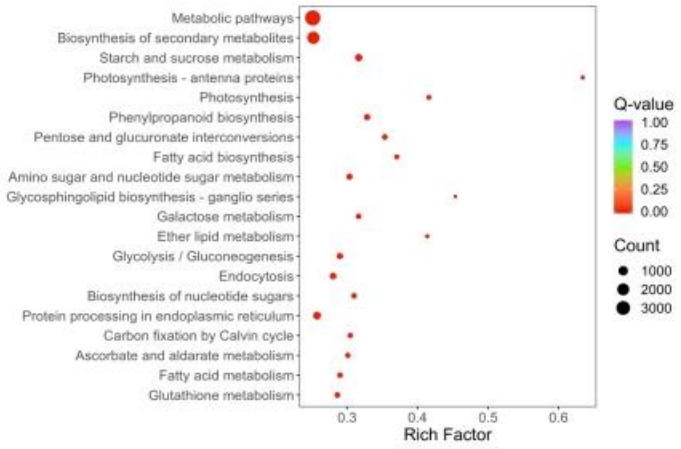

(f)

Figure 2. Functional enrichment analysis of differentially expressed genes during inflorescence development in *Agropyron cristatum*. **(a-c)** Gene Ontology enrichment analysis of DEGs in the HS_vs_BS, FS_vs_HS, and FS_vs_BS comparisons, respectively. **(d-f)** KEGG pathway enrichment analysis of DEGs in the HS_vs_BS, FS_vs_HS, and FS_vs_BS comparisons, respectively.

- Metabolomic Analysis

To quantify phytohormone levels during three developmental stages of the inflorescence, we performed targeted phytohormone metabolomic analysis. Subsequently, in the comparisons of HS_vs_BS, FS_vs_HS, and FS_vs_BS, we identified 14, 28, and 31 differentially accumulated metabolites (DAMs), respectively (Figure 3). Moreover, differential accumulation was observed across the three comparison groups for seven phytohormone classes, including gibberellins (GA), auxins (IAA), cytokinins (CK), jasmonates (JA), salicylic acid (SA), and abscisic acid (ABA). These results indicate that these phytohormones are likely involved in floret bud development.

In the HS_vs_BS comparison, two GAs showed significant upregulation: GA29 ($Log_2FC = 5.69$) and GA53 ($Log_2FC = Inf$). In contrast, in the FS_vs_HS comparison, GA19 ($Log_2FC = -Inf$) was significantly downregulated.

For auxins, one compound, TRA ($Log_2FC = 1.07$), was significantly upregulated in HS_vs_BS, while two auxins, TRP ($Log_2FC = -1.46$) and IAA-Glu ($Log_2FC = Inf$), were downregulated. In FS_vs_HS, multiple auxins were significantly upregulated, including IAA ($Log_2FC = 3.37$), TRP ($Log_2FC = 1.11$), MEIAA ($Log_2FC = 1.51$), ICA ($Log_2FC = 1.40$), IAA-Asp ($Log_2FC = 7.17$), IAA-Phe ($Log_2FC = Inf$), and OxIAA ($Log_2FC = Inf$), whereas ICAld ($Log_2FC = -Inf$) was downregulated.

Regarding cytokinins (CK), iP9G ($Log_2FC = 2.42$), IP ($Log_2FC = 1.39$), cZR ($Log_2FC = Inf$), and KR ($Log_2FC = Inf$) were significantly upregulated in HS_vs_BS, whereas DHZ7G ($Log_2FC = -Inf$), tZ ($Log_2FC = -Inf$), tZRMP ($Log_2FC = -Inf$), and cZRMP ($Log_2FC = -Inf$) were downregulated. Strikingly, in the FS_vs_HS comparison, all detected CK metabolites exhibited a significant upregulation trend, including iPRMP ($Log_2FC = 1.02$), 2MeScZR ($Log_2FC = 1.13$), IPR ($Log_2FC = 2.36$), iP9G ($Log_2FC = 3.99$), iP7G ($Log_2FC = 2.97$), IP ($Log_2FC = 5.93$), DHZROG ($Log_2FC = 3.36$), tZ9G ($Log_2FC = 2.31$), DHZ7G ($Log_2FC = Inf$), tZ ($Log_2FC = Inf$), tZRMP ($Log_2FC = Inf$), tZR ($Log_2FC = Inf$), 2MeSiP ($Log_2FC = Inf$), and K9G ($Log_2FC = Inf$).

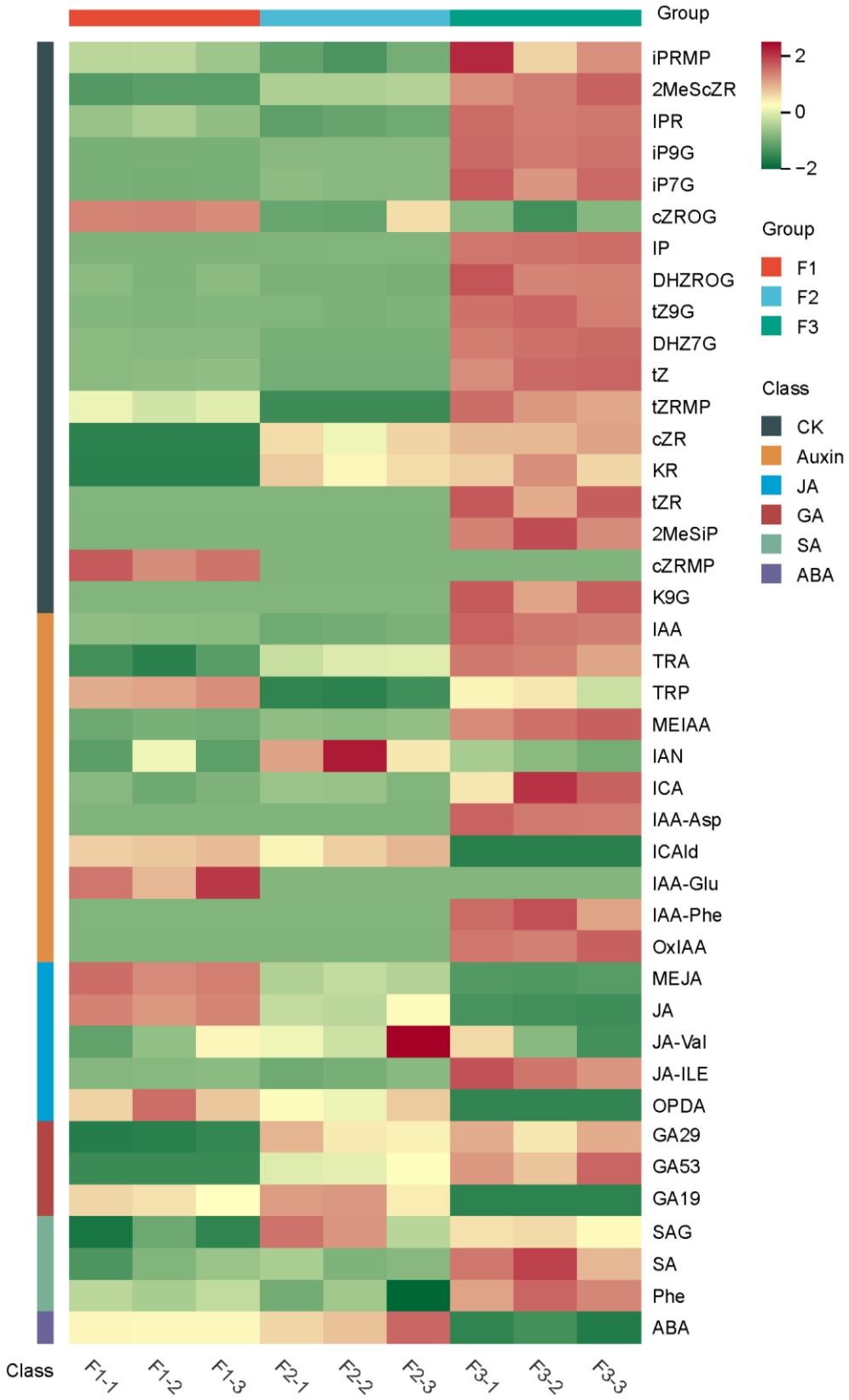

Figure 3. Heatmap depicting the accumulation dynamics of key phytohormones and their metabolites across three inflorescence developmental stages.

- Transcriptomic Analysis of Genes Involved in Phytohormone Biosynthesis and Signal Transduction

Key genes involved in the biosynthesis pathways of GA, IAA, and CK

To elucidate the underlying molecular mechanisms, we analyzed the dynamic expression patterns of genes involved in major phytohormone signaling pathways, including GA, IAA, and CK.

In the GA biosynthesis pathway (Figure 4a), we found that two KS genes (Cluster-29851.6; Cluster-86843.7) and one KAO gene (Cluster-97084.1) were differentially expressed in the HS_vs_BS comparison. In the FS_vs_HS comparison, one CPS (Cluster-91802.1), seven KS genes (Cluster-13804.0, Cluster-29851.4, Cluster-29851.6, Cluster-29851.7, Cluster-29851.9, Cluster-86843.4, Cluster-86843.7), two GA13ox genes (Cluster-84143.0, Cluster-84143.1), two GA44ox genes (Cluster-38874.8, Cluster-57501.0), eight GA2ox genes (Cluster-14948.0, Cluster-24676.2, Cluster-24676.3, Cluster-24676.4, Cluster-24676.6, Cluster-24676.7, Cluster-48006.0, Cluster-93569.0), and two GA3ox genes (Cluster-82607.0, Cluster-90263.0) were significantly differentially expressed.

In the IAA biosynthesis pathway (Figure 4b), we identified one TDC (Cluster-50033.0), five AO1 genes (Cluster-66214.0, Cluster-66214.12, Cluster-66214.14, Cluster-66214.15, Cluster-66214.21), twelve ALDH genes (Cluster-57069.14, Cluster-57069.3, Cluster-63906.1, Cluster-79950.2, Cluster-79950.6, Cluster-91034.1, Cluster-91034.5, Cluster-91034.6, Cluster-91034.8, Cluster-93368.15, Cluster-93368.4, Cluster-93973.0), five YUCCA genes (Cluster-19893.3, Cluster-91666.0, Cluster-91666.3, Cluster-91666.8, Cluster-95273.1), and seven amid genes (Cluster-84647.0, Cluster-84647.5, Cluster-84647.6, Cluster-94913.1, Cluster-94913.2, Cluster-94913.4, Cluster-94913.5) as differentially expressed in the HS_vs_BS comparison. In the FS_vs_HS comparison, three TDC genes (Cluster-52760.89, Cluster-50033.0, Cluster-66035.0), four TAA1 genes (Cluster-16838.0, Cluster-16838.1, Cluster-16838.2, Cluster-16838.3), eight YUCCA genes (Cluster-15379.0, Cluster-15705.0, Cluster-41163.0, Cluster-3016.7, Cluster-72122.0, Cluster-91666.5, Cluster-95056.10, Cluster-95056.12), ten ALDH genes (Cluster-79950.2, Cluster-79950.6, Cluster-91034.2, Cluster-91034.3, Cluster-91034.6, Cluster-91034.8, Cluster-93368.11, Cluster-93368.14, Cluster-93368.15, Cluster-93973.0), and sixteen amid genes (Cluster-14048.0, Cluster-67371.10, Cluster-67371.13, Cluster-67371.14, Cluster-67371.6, Cluster-84647.0, Cluster-84647.5, Cluster-84647.6, Cluster-85259.12, Cluster-92542.0, Cluster-92542.2, Cluster-92542.5, Cluster-94913.1, Cluster-94913.2, Cluster-94913.4, Cluster-94913.5) were significantly differentially expressed.

In the CK biosynthesis pathway (Figure 4c), one miaA gene (Cluster-93939.3) was differentially expressed in the HS_vs_BS comparison, and nine IPT genes (Cluster-13576.0, Cluster-13576.1, Cluster-21829.0, Cluster-55586.0, Cluster-55586.2, Cluster-55586.5, Cluster-55586.6, Cluster-76954.0, Cluster-96297.0) were differentially expressed in the FS_vs_HS comparison.

We performed a comparative analysis of the transcriptional dynamics of differentially expressed genes (DEGs) within the GA, IAA, and CK biosynthesis pathways across different developmental comparisons (Figure 4). The results revealed that in the GA pathway, the HS_vs_BS comparison showed 2 up-regulated and 4 down-regulated genes, while the FS_vs_HS comparison exhibited 21 up-regulated and 1 down-regulated genes. In the IAA pathway, the HS_vs_BS comparison contained 29 up-regulated and 1 down-regulated genes, and the FS_vs_HS comparison displayed 9 up-regulated genes and 32 down-regulated genes. For the CK pathway, the HS_vs_BS comparison included 1 down-regulated genes, whereas the FS_vs_HS comparison had 9 up-regulated.

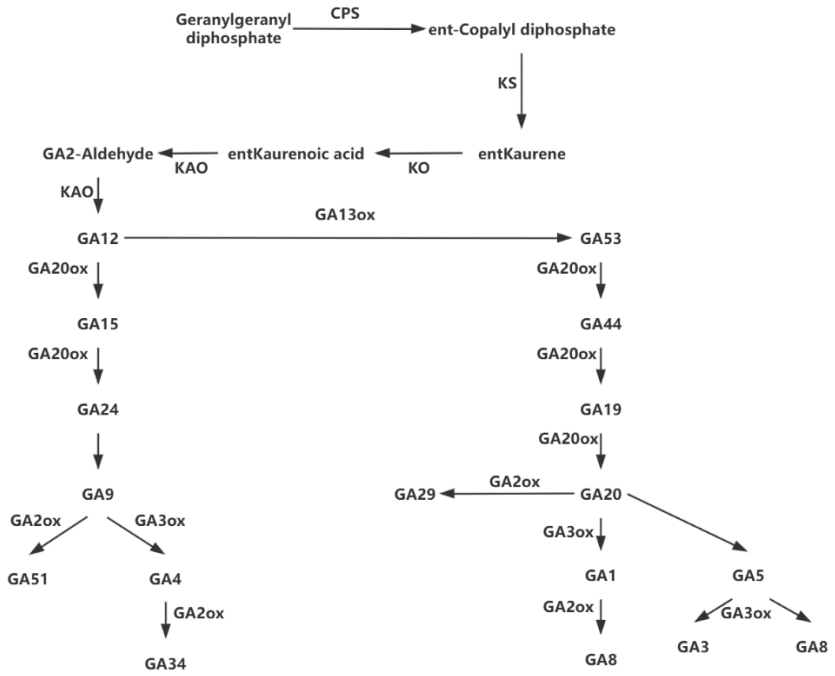
Geranylgeranyl diphosphate
CPS
ent-Copalyl diphosphate
KS
entKaurene
KO
entKaurenoic acid
KAO
GA2-Aldehyde
KAO
GA13ox
GA12
GA53
GA20ox
GA15
GA44
GA24
GA19
GA9
GA29
GA2ox
GA20
GA3ox
GA2ox
GA51
GA4
GA1
GA5
GA2ox
GA3ox
GA34
GA8
GA3
GA8

(a)

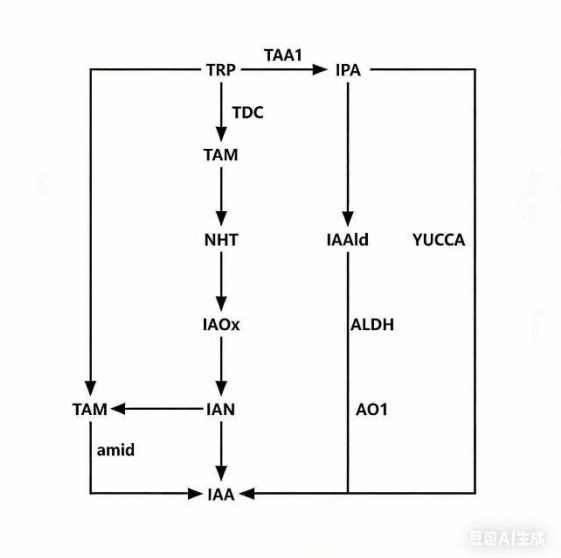
TRP
TAA1
IPA
TDC
TAM
NHT
IAAld
YUCCA
IAOx
ALDH
TAM
IAN
AO1
amid
IAA

(b)

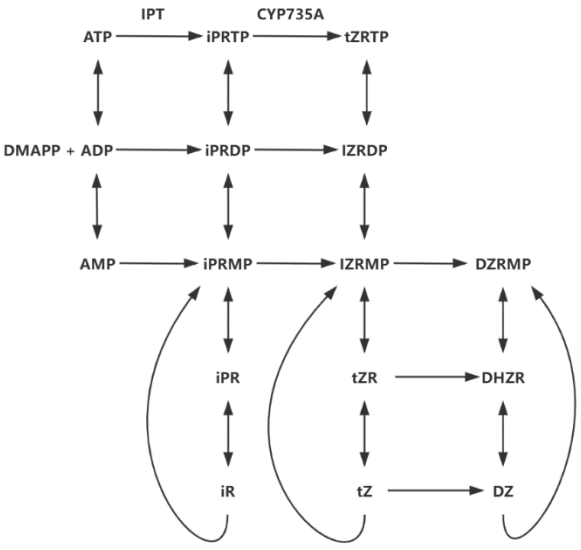
IPT
CYP735A
ATP
iPRTP
tZRTP
DMAPP + ADP
iPRDP
IZRDP
AMP
iPRMP
IZRMP
DZRMP
iPR
tZR
DHZR
iR
tZ
DZ

(c)

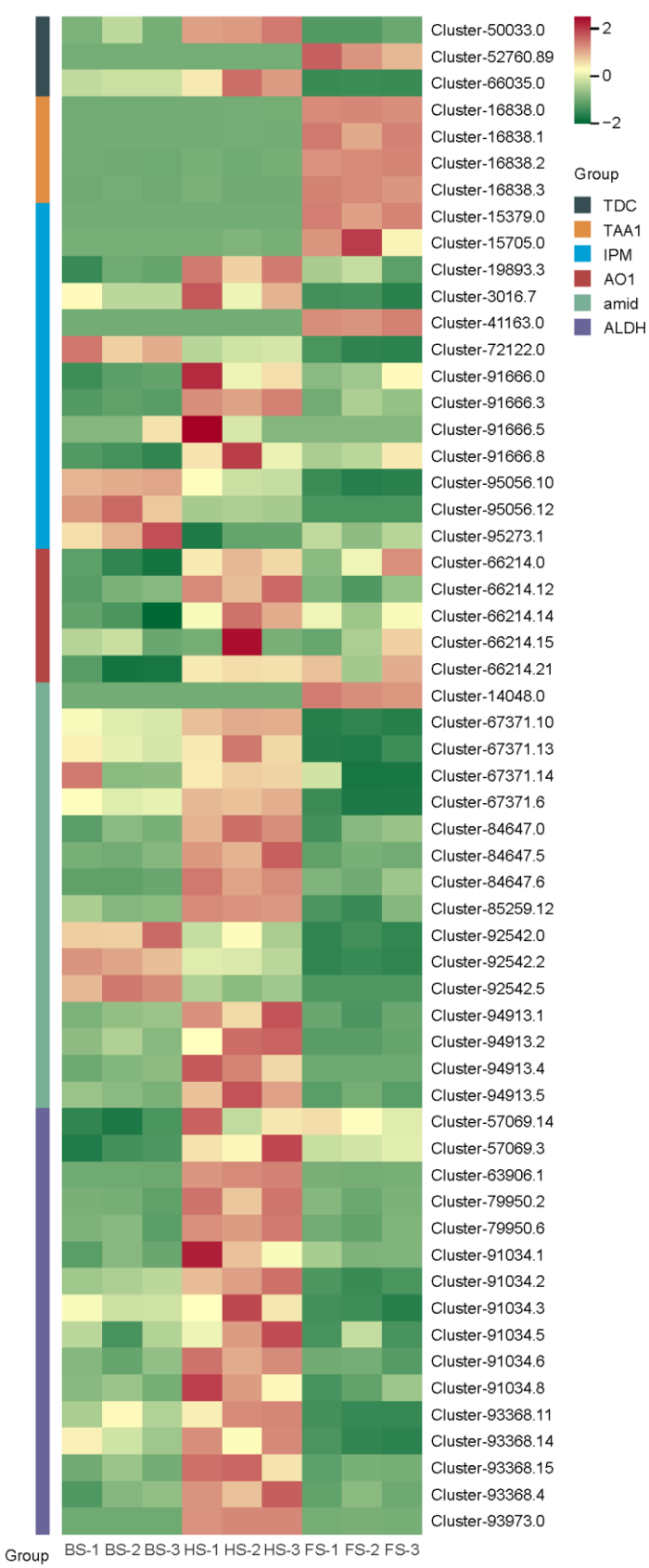
Cluster-50033.0
Cluster-52760.89
Cluster-66035.0
Cluster-16838.0
Cluster-16838.1
Cluster-16838.2
Cluster-16838.3
Cluster-15379.0
Cluster-15705.0
Cluster-19893.3
Cluster-3016.7
Cluster-41163.0
Cluster-72122.0
Cluster-91666.0
Cluster-91666.3
Cluster-91666.5
Cluster-91666.8
Cluster-95056.10
Cluster-95056.12
Cluster-95273.1
Cluster-66214.0
Cluster-66214.12
Cluster-66214.14
Cluster-66214.15
Cluster-66214.21
Cluster-14048.0
Cluster-67371.10
Cluster-67371.13
Cluster-67371.14
Cluster-67371.6
Cluster-84647.0
Cluster-84647.5
Cluster-84647.6
Cluster-85259.12
Cluster-92542.0
Cluster-92542.2
Cluster-92542.5
Cluster-94913.1
Cluster-94913.2
Cluster-94913.4
Cluster-94913.5
Cluster-57069.14
Cluster-57069.3
Cluster-63906.1
Cluster-79950.2
Cluster-79950.6
Cluster-91034.1
Cluster-91034.2
Cluster-91034.3
Cluster-91034.5
Cluster-91034.6
Cluster-91034.8
Cluster-93368.11
Cluster-93368.14
Cluster-93368.15
Cluster-93368.4
Cluster-93973.0
2
0
−2
Group
TDC
TAA1
IPM
AO1
amid
ALDH
Group
BS-1 BS-2 BS-3 HS-1 HS-2 HS-3 FS-1 FS-2 FS-3

(e)

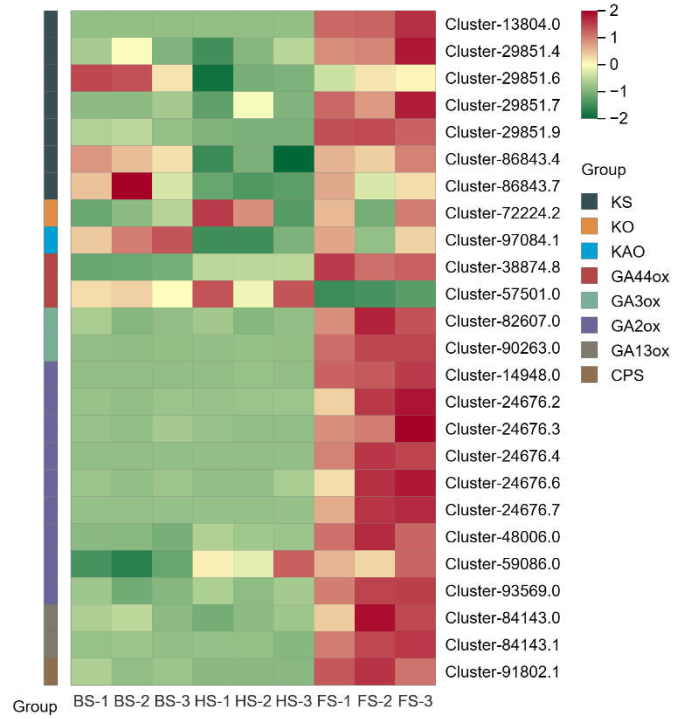
Cluster-13804.0
Cluster-29851.4
Cluster-29851.6
Cluster-29851.7
Cluster-29851.9
Cluster-86843.4
Cluster-86843.7
Cluster-72224.2
Cluster-97084.1
Cluster-38874.8
Cluster-57501.0
Cluster-82607.0
Cluster-90263.0
Cluster-14948.0
Cluster-24676.2
Cluster-24676.3
Cluster-24676.4
Cluster-24676.6
Cluster-24676.7
Cluster-48006.0
Cluster-59086.0
Cluster-93569.0
Cluster-84143.0
Cluster-84143.1
Cluster-91802.1
2
1
0
−1
−2
Group
KS
KO
KAO
GA44ox
GA3ox
GA2ox
GA13ox
CPS
Group
BS-1 BS-2 BS-3 HS-1 HS-2 HS-3 FS-1 FS-2 FS-3

(d)


Cluster-93939.3
Cluster-13576.0
Cluster-13576.1
Cluster-21829.0
Cluster-55586.0
Cluster-55586.2
Cluster-55586.5
Cluster-55586.6
Cluster-76954.0
Cluster-96297.0
2
1
0
−1
Group
miaA
IPT
Group
BS-1 BS-2 BS-3 HS-1 HS-2 HS-3 FS-1 FS-2 FS-3

(f)

Figure 4. Schematic diagrams of key phytohormone biosynthesis pathways. **(a)** GA biosynthesis pathway; **(b)** IAA biosynthesis pathway; **(c)** CK biosynthesis pathway. **(d)** Clustering heatmap of differentially expressed genes in the GA biosynthesis pathway. **(e)** Clustering heatmap of differentially expressed genes in the IAA biosynthesis pathway. **(f)** Clustering heatmap of differentially expressed genes in the CK biosynthesis pathway.

Key genes involved in the signaling pathways of GA, IAA, and CK

In the GA signal transduction pathway, one GID1 (Cluster-72442.0), one DELLA (Cluster-21168.0), and seven TFs (Cluster-71900.11, Cluster-85384.0, Cluster-95947.6, Cluster-96020.2, Cluster-54197.0, Cluster-17030.2, Cluster-94689.4) were differentially expressed in the HS_vs_BS, FS_vs_HS, and FS_vs_BS comparisons.

In the IAA signal transduction pathway, one AUX1/LAX (Cluster-70497.2), one TIR1 (Cluster-93838.3), one ARF (Cluster-82530.3), two GH3s (Cluster-46829.0, Cluster-56921.0), and three SAURs (Cluster-64974.1, Cluster-84714.0, Cluster-90414.15) were differentially expressed in the HS_vs_BS, FS_vs_HS, and FS_vs_BS comparisons.

In the CK signal transduction pathway, two CRE1s (Cluster-24313.0, Cluster-79434.0) and five B-ARRs (Cluster-64858.1, Cluster-64987.0, Cluster-71214.0, Cluster-87606.0, Cluster-91549.3) were differentially expressed in the HS_vs_BS, FS_vs_HS, and FS_vs_BS comparisons.

We conducted a comparative analysis of the transcriptional dynamics of DEGs within the GA, IAA, and CK biosynthesis pathways across developmental comparisons (Figure 5). The results indicated that in the GA pathway, the HS_vs_BS comparison contained 13 up-regulated and 3 down-regulated genes, while the FS_vs_HS comparison exhibited 11 up-regulated and 23 down-regulated genes. In the IAA pathway, the HS_vs_BS comparison showed 9 up-regulated and 7 down-regulated genes, and the FS_vs_HS comparison displayed 23 up-regulated and 18 down-regulated genes. Regarding the CK pathway, the HS_vs_BS comparison included 8 up-regulated and 4 down-regulated genes, whereas the FS_vs_HS comparison had 12 up-regulated and 16 down-regulated genes.

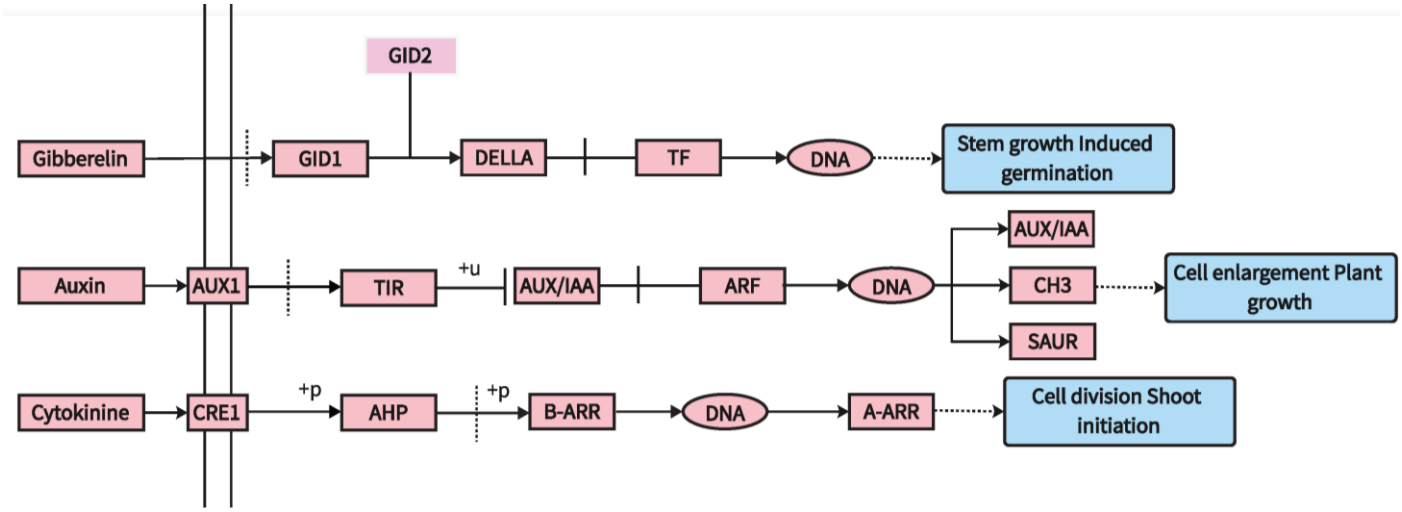
GID2
Gibberelin
GID1
DELLA
TF
DNA
Stem growth Induced germination
Auxin
AUX1
TIR
+u
AUX/IAA
ARF
DNA
AUX/IAA
CH3
SAUR
Cell enlargement Plant growth
Cytokinine
CRE1
+p
AHP
+p
B-ARR
DNA
A-ARR
Cell division Shoot initiation

(**a**)

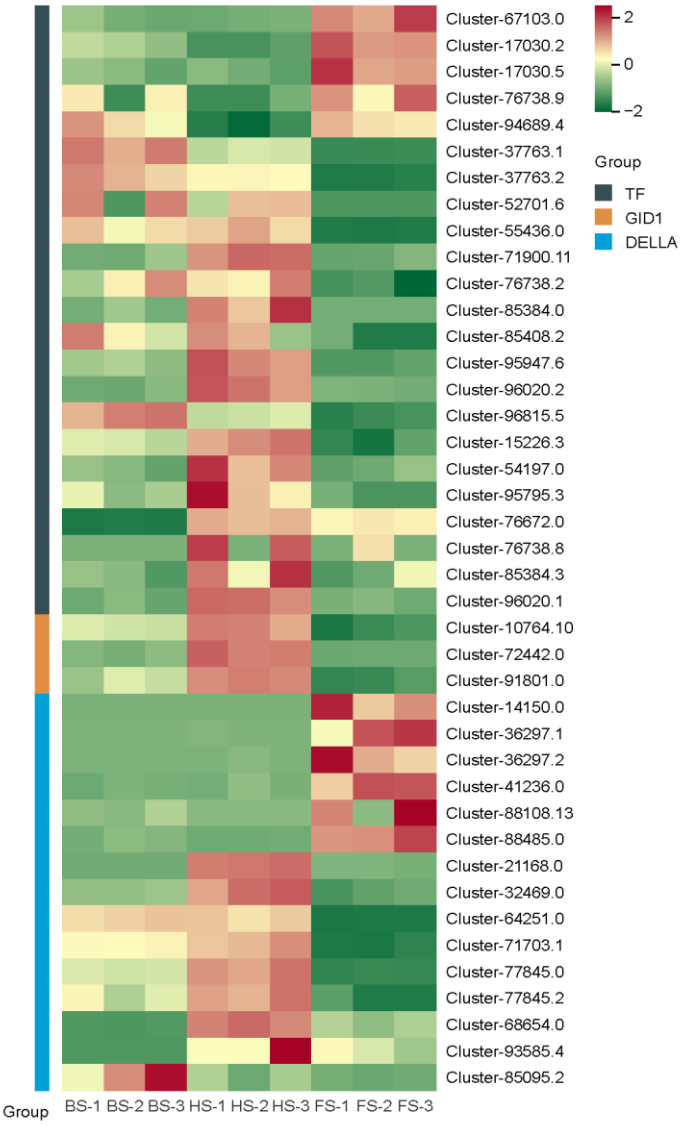
Cluster-67103.0
Cluster-17030.2
Cluster-17030.5
Cluster-76738.9
Cluster-94689.4
Cluster-37763.1
Cluster-37763.2
Cluster-52701.6
Cluster-55436.0
Cluster-71900.11
Cluster-76738.2
Cluster-85384.0
Cluster-85408.2
Cluster-95947.6
Cluster-96020.2
Cluster-96815.5
Cluster-15226.3
Cluster-54197.0
Cluster-95795.3
Cluster-76672.0
Cluster-76738.8
Cluster-85384.3
Cluster-96020.1
Cluster-10764.10
Cluster-72442.0
Cluster-91801.0
Cluster-14150.0
Cluster-36297.1
Cluster-36297.2
Cluster-41236.0
Cluster-88108.13
Cluster-88485.0
Cluster-21168.0
Cluster-32469.0
Cluster-64251.0
Cluster-71703.1
Cluster-77845.0
Cluster-77845.2
Cluster-68654.0
Cluster-93585.4
Cluster-85095.2
2
0
−2
Group
TF
GID1
DELLA
Group
BS-1 BS-2 BS-3 HS-1 HS-2 HS-3 FS-1 FS-2 FS-3

(**b**)

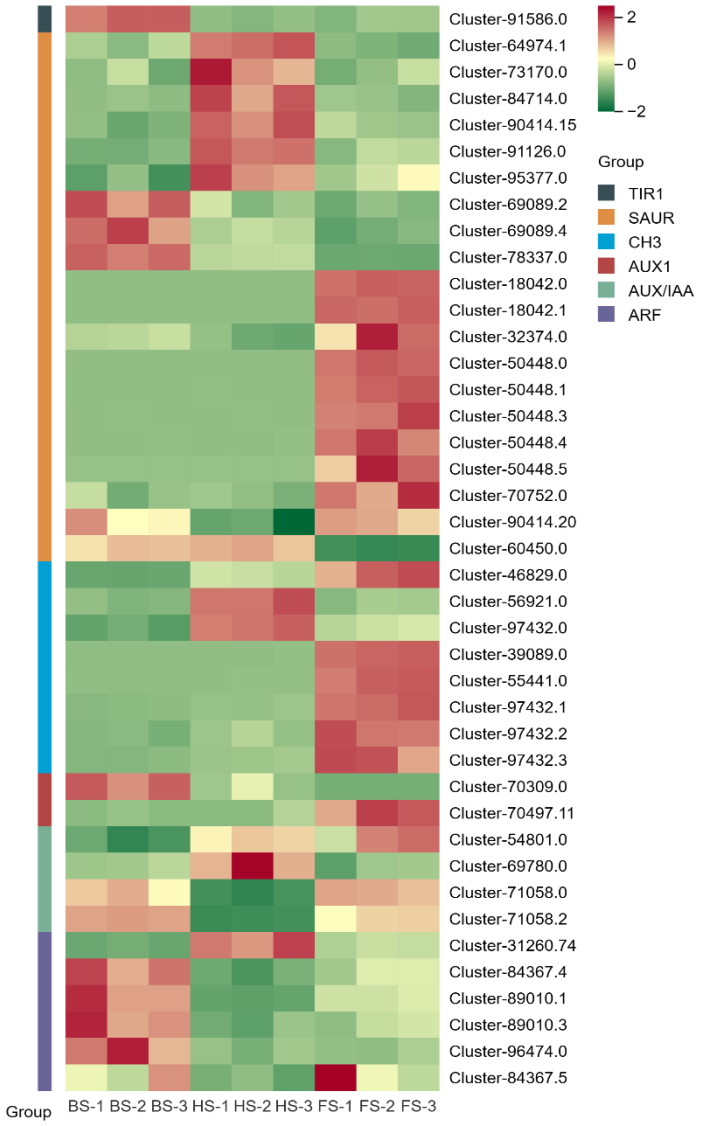
Cluster-91586.0
Cluster-64974.1
Cluster-73170.0
Cluster-84714.0
Cluster-90414.15
Cluster-91126.0
Cluster-95377.0
Cluster-69089.2
Cluster-69089.4
Cluster-78337.0
Cluster-18042.0
Cluster-18042.1
Cluster-32374.0
Cluster-50448.0
Cluster-50448.1
Cluster-50448.3
Cluster-50448.4
Cluster-50448.5
Cluster-70752.0
Cluster-90414.20
Cluster-60450.0
Cluster-46829.0
Cluster-56921.0
Cluster-97432.0
Cluster-39089.0
Cluster-55441.0
Cluster-97432.1
Cluster-97432.2
Cluster-97432.3
Cluster-70309.0
Cluster-70497.11
Cluster-54801.0
Cluster-69780.0
Cluster-71058.0
Cluster-71058.2
Cluster-31260.74
Cluster-84367.4
Cluster-89010.1
Cluster-89010.3
Cluster-96474.0
Cluster-84367.5
2
0
−2
Group
TIR1
SAUR
CH3
AUX1
AUX/IAA
ARF
Group
BS-1 BS-2 BS-3 HS-1 HS-2 HS-3 FS-1 FS-2 FS-3

(**c**)

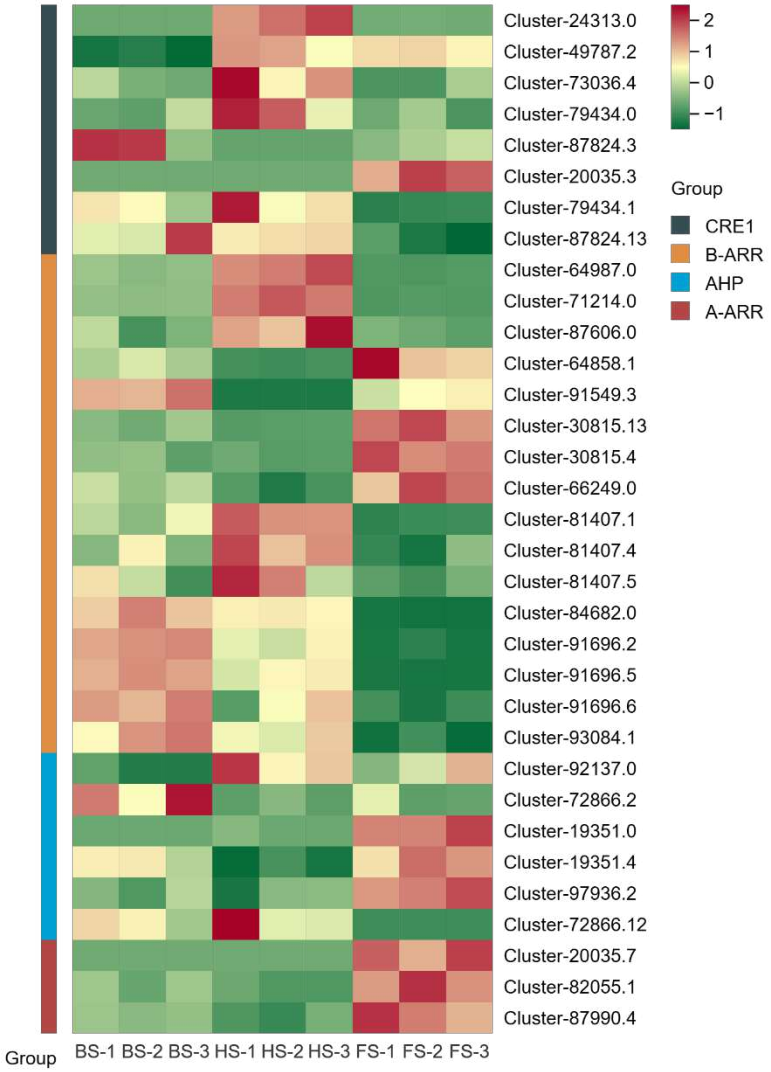

(**d**)

Figure 5. **(a)** Schematic Diagram of Major Plant Hormone Signaling Pathways: Gibberellin, Auxin, and Cytokinin. **(b)** Schematic diagram of differentially expressed genes in the GA signaling pathway. **(c)** Clustering heatmap of differentially expressed genes in the IAA signaling pathway. **(d)** Clustering heatmap of differentially expressed genes in the CK signaling pathway.

Transcription Factor Analysis

Several transcription factor families associated with floral development were identified in this study, such as AP2/ERF-ERF, MYB, TCP, HD-ZIP, WOX, LFY, and NF-YC. Across the three comparison groups, a total of 2,059 transcription factors were identified, including 93 (4.52%) belonging to the AP2/ERF-ERF family, 65 (3.16%) to the MYB family, 19 (0.92%) to the TCP family, 18 (0.87%) to the HD-ZIP family, 3 (0.15%) to the WOX family, 1 (0.05%) to the LFY family, and 14 (0.68%) to the NF-YC family, suggesting these families may play significant roles in regulating inflorescence growth.

Further analysis revealed that among the differentially expressed transcription factors, 43 exhibited consistent up-regulation across all three developmental stages. These include: 1 AP2/ERF-ERF, 3 B3, 1 bHLH, 5 bZIP, 2 C2C2-GATA, 5 C2H2, 1 C3H, 1 CPP, 1 FAR1, 1 LOB, 2 MADS-M-type, 4 MADS-MIKC, 3 MYB, 4 MYB-related, 2 NAC, 1 OFP, 1 PLATZ, 1 SND2, 1 TAZ, and 1 Tify. Concurrently, 13 transcription factors showed consistent down-regulation across the three stages, including: 2 AP2/ERF-AP2, 1 AP2/ERF-ERF, 1 AUX/IAA, 3 B3, 2 B3-ARF, 2 bHLH, 2 C2C2-Dof, 1 C2C2-GATA, 1 C2C2-YABBY, 2 FAR1, 3 HB-HD-ZIP, 1 HB-KNOX, 1 HSF, 4 MYB, 1 NAC, 1 NF-YA, 1 NF-YB, 1 OFP, 4 SBP, 1 SET, 3 TCP, 4 WRKY, and

1 zf-HD. These transcription factors with sustained expression changes are likely closely associated with the process of inflorescence development.

Discussion

GA primarily regulates inflorescence architecture by promoting the establishment and elongation of the inflorescence meristem. Its signaling pathway mediates the degradation of *DELLA* proteins, thereby releasing the inhibition on growth-promoting factors and regulating rachis elongation as well as floral organ initiation and development [28]. In rice, mutations in key genes of GA biosynthesis or signaling lead to typical phenotypes such as shortened panicles and reduced grain number per panicle [29]. In Arabidopsis, GA precisely promotes the transition from the shoot apical meristem to the inflorescence meristem and maintains its activity for floret primordia formation during developmental timing [30]. Correspondingly, in wheat, exogenous GA application has been shown to induce spike development under short-day conditions within specific genetic backgrounds, collectively affirming GA's conserved and crucial role as an endogenous signal driving inflorescence initiation and development [31]. As a key rate-limiting enzyme in early GA biosynthesis, loss-of-function mutants of *KO* result in a blocked synthesis pathway, significantly reducing endogenous active GA levels and causing extreme dwarfism and other typical phenotypes [32]. Transcriptomic data from this study show that *KO* gene expression was upregulated in both the HS_vs_BS and FS_vs_HS comparisons, suggesting its potential role in promoting early GA biosynthesis and facilitating the accumulation of GA precursors. Furthermore, among the differentially expressed genes in FS_vs_HS, we identified multiple highly expressed key enzyme genes in the GA metabolic pathway, including: *KS* (4), *GA13ox* (2), *GA44ox* (1), *GA2ox* (8), and *GA3ox* (1). These expression changes collectively indicate that GA synthesis, activation, and inactivation metabolism are transcriptionally regulated at multiple levels across different stages of inflorescence development. This dynamic balance may directly influence the final GA levels and signal output, thereby regulating inflorescence morphogenesis. IAA plays a central role in inflorescence development through its polar and local distribution, which establishes positional signals for morphogenesis. Its transport network, formed by PIN-family proteins in the apical meristem, determines the initiation sites of floral primordia and organ patterning, such as the maintenance and differentiation of spikelet meristems [33]. Research indicates that auxin response factors directly regulate downstream target genes, serving as key nodes controlling inflorescence branching and floral organ development [34]. YUCCA proteins are flavin monooxygenases; their overexpression leads to significantly elevated IAA levels in plants, resulting in a high-auxin phenotype [35]. Transcriptomic data from this study show that in both the HS_vs_BS and FS_vs_HS comparisons, three *YUCCA* family genes were up-regulated and highly expressed, indicating that the key rate-limiting step of auxin biosynthesis was significantly activated between the comparison groups. Further analysis revealed significant expression changes in other critical genes of the auxin synthesis pathway: in HS_vs_BS, *TDC* (1), *AO1* (4), and *ALDH* (7) genes were significantly highly expressed; whereas in FS_vs_HS, *TAA1* (4) and one *amid* gene showed high expression. These genes are involved in different stages of auxin synthesis, including precursor supply, intermediate metabolism, and final product formation. Their coordinated up-regulation suggests that they may collectively contribute to promoting the accumulation of endogenous IAA during corresponding developmental stages or under specific conditions. CK functions to maintain the cell division activity of meristems and prevent their premature differentiation. Higher CK levels contribute to enlarging the meristem and increasing the number of organ primordia, which in cereal crops directly translates into more spikelets or branches [36]. For example, loss of function of the *OsCKX2* gene, which encodes a cytokinin oxidase in rice, leads to CK accumulation in the inflorescence meristem, significantly increasing the number of secondary branches and grains [37]. Conversely, loss of function of *IPT* genes results in a marked decrease in CK content in plants [38]. In this study, within the FS_vs_HS comparison, all nine *IPT* genes were significantly up-regulated, potentially associated with CK accumulation. This transcriptomic finding aligns with and is corroborated by the non-targeted metabolomic data from this study.

GA signaling primarily drives the rapid elongation of the inflorescence axis and maintains meristem activity by relieving the repression of downstream transcription factors by DELLA proteins. It serves as a key initiation signal for the transition from vegetative to reproductive growth [39]. In this study, the higher expression levels of *DELLA* down-regulated genes during the FS stage indicate that *DELLA* proteins play a crucial role in inflorescence development.IAA signaling determines the boundary specification of floral organs and acts as a core instruction for the patterning of inflorescence structure [40]. In this study, most genes of the *AUX/IAA*, *GH3*, and *SAUR* families maintained high expression levels.CK signaling is transmitted through a two-component system. Its core function is to maintain stem cell activity in the meristem and inhibit premature differentiation. Higher CK signaling levels help expand meristem capacity and increase the number of floral organ primordia, directly influencing inflorescence complexity and seed-setting potential [25, 41]. The high expression pattern of *B-ARR* across both the HS and FS stages suggests its potentially important regulatory role in inflorescence development.

The development of plant inflorescences is coordinately regulated by multiple layers of transcription factors, forming a complex molecular regulatory network. The AP2/ERF family plays a central role in the photoperiodic response of rice inflorescences; for example, its member LFS directly binds to and represses the expression of the flowering suppressor gene *OsLFL1*, thereby regulating flowering time under long-day conditions [42]. MYB transcription factors influence inflorescence architecture by integrating hormonal signals. In Arabidopsis, MYB21/MYB24 interact with JAZ proteins in the jasmonate pathway to directly regulate stamen development [43]. The TCP family is a key architect of inflorescence

morphological diversity: CYC-class members regulate floral symmetry and floral form evolution [44]; whereas AtTCP7, AtTCP8, and AtTCP15 positively regulate flowering by directly activating the expression of the flowering integrator *SOC1* [45-47]; TB1 and its orthologs collectively determine inflorescence compactness and morphology by suppressing lateral branching or regulating floral organ development [48]. HD-ZIP Class I members, such as barley HvHOX1/VRS1, specifically suppress lateral spikelet development to determine inflorescence row number, and its paralog HvHOX2 exhibits functional redundancy in this process [49]. The WOX family is indispensable for meristem function maintenance; for instance, multiple WUS-clade genes are highly expressed in the inflorescence meristem of sunflower, directly participating in floral initiation and inflorescence structure establishment [50]. LFY is a key determinant of floral meristem identity; it activates the expression of floral homeotic genes, driving the transition of floral organ identity from vegetative to reproductive and ensuring normal floral organ development [51]. Additionally, the NF-Y complex participates in photoperiodic flowering regulation; the nuclear factors NF-YB2 and NF-YC9 interact with the core photoperiodic regulator CO to cooperatively activate the expression of the florigen gene *FT*, thereby regulating the floral transition [52]. In summary, these transcription factors collectively orchestrate the entire process of plant inflorescence development through precise and interconnected regulatory mechanisms. We identified several key transcription factors closely associated with floral organ and inflorescence development, including AP2/ERF-ERF, MYB, TCP, HD-ZIP, WOX, LFY, and NF-YC. The up-regulation or down-regulation of these transcription factors during development may directly influence inflorescence meristem activity, floral organ initiation and differentiation, thereby regulating the final morphology and structural establishment of the inflorescence.

Methods

- Plant Materials

This study utilized Agropyron cristatum as the plant material, and the experiment was conducted at the Germplasm Resource Nursery of the Grassland Research Institute, Chinese Academy of Agricultural Sciences (40.6°N, 111.8°E). During the 2025 growing season, samples were precisely collected at three key developmental stages of inflorescence: booting stage, heading stage, and flowering stage. For each stage, five healthy and disease-free plants were randomly selected from each biological replicate plot, and the complete apical inflorescence from the main stem of each plant was excised. Immediately after collection, the samples were flash-frozen in liquid nitrogen for 10 minutes and subsequently transferred to a -80°C freezer for long-term storage, to be used for subsequent transcriptome sequencing, endogenous hormone quantification, and gene expression analysis.

- Phytohormone Analysis

Endogenous GA, IAA, CK, JA, SA and ABA were quantified via LC–MS/MS. Briefly, 15 mg samples were extracted with 1 mL methanol/water/formic acid (15:4:1, v/v/v), spiked with 10 μL 100 ng/mL internal standard mixture, vortexed 10 min, centrifuged at 12,000 r/min for 5 min (4 °C), then the supernatant was evaporated, re-dissolved in 100 μL 80% methanol, filtered prior to analysis. UPLC and ESI-MS/MS conditions followed Jan Šimura et al.[53].

- RNA-Seq

Samples were precisely collected at three key stages of inflorescence development (booting, heading, and flowering). For each stage, five healthy, disease-free plants were randomly selected from each biological replicate plot, and the intact terminal inflorescence on the main stem was excised from each plant. After collection, the samples were immediately snap-frozen in liquid nitrogen for 10 minutes and then stored at −80 °C. Transcriptome sequencing was conducted by Metware Biotechnology Co., Ltd. (Wuhan, China).

- Weighted Gene Co-Expression Network Analysis

Weighted gene co-expression network analysis (WGCNA) was performed using the R package (v4.3.0). An unsigned topological overlap measure was adopted for network construction and module identification across the dataset, with parameters set as follows: minimum module size of 30, merge cut height of 0.25, and soft-threshold power enabled. Intramodular connectivity was calculated to prioritize genes within each module, and the top 15 hub genes were selected. The Pearson correlation coefficient (PCC) was employed to evaluate module-level associations. Visualization of the identified modules was conducted using Cytoscape v3.7.1 [54].

- qRT-PCR

The expression patterns of DEGs identified by RNA sequencing were further validated via quantitative real-time PCR (qRT-PCR). Eight DEGs were randomly selected for transcriptional validation with gene-specific primers (Figure S1). qRT-PCR assays verified that all selected genes displayed stage-specific differential expression across the BS, HS and FS of inflorescence development.

References

1. Said M, Parada AC, Gaál E, Molnár I, Cabrera A, Doležel J, et al. Uncovering homeologous relationships between tetraploid *Agropyron cristatum* and bread wheat genomes using COS markers. Theor Appl Genet. 2019;132(10):2881-98.
2. Pan C, Li Q, Han H, Zhang J, Zhou S, Yang X, et al. Identification of 5P Chromosomes in Wheat-*Agropyron cristatum* Addition Line and Analysis of Its Effect on Homologous Pairing of Wheat Chromosomes. Front Plant Sci. 2022;13:844348.
3. Zhang Z, Zhou S, Liu W, Song L, Zhang J, Han H, et al. Molecular Cytogenetic Analysis of the Introgression between *Agropyron cristatum* P Genome and Wheat Genome. Int J Mol Sci. 2021;22(20).
4. Qi K, Han H, Zhang J, Zhou S, Li X, Yang X, et al. Development and characterization of novel Triticum aestivum-*Agropyron cristatum* 6P Robertsonian translocation lines. Mol Breed. 2021;41(10):59.
5. Lu M, Lu Y, Li H, Pan C, Guo Y, Zhang J, et al. Transferring Desirable Genes from *Agropyron cristatum* 7P Chromosome into Common Wheat. PLoS One. 2016;11(7):e0159577.
6. Han H, Liu W, Zhang J, Zhou S, Yang X, Li X, et al. Identification of P genome chromosomes in *Agropyron cristatum* and wheat-A. cristatum derivative lines by FISH. Sci Rep. 2019;9(1):9712.
7. Han H, Yang J, Qi K, Zhu H, Wu P, Zhou S, et al. Introgression of chromosome 5P from *Agropyron cristatum* enhances grain weight in a wheat background. Theor Appl Genet. 2024;137(7):165.
8. Song L, Lu Y, Zhang J, Pan C, Yang X, Li X, et al. Physical mapping of *Agropyron cristatum* chromosome 6P using deletion lines in common wheat background. Theor Appl Genet. 2016;129(5):1023-34.
9. Wang X, Han B, Sun Y, Kang X, Zhang M, Han H, et al. Introgression of chromosome 1P from *Agropyron cristatum* reduces leaf size and plant height to improve the plant architecture of common wheat. Theor Appl Genet. 2022;135(6):1951-63.
10. Ford-Lloyd BV, Schmidt M, Armstrong SJ, Barazani O, Engels J, Hadas R, et al. Crop Wild Relatives—Undervalued, Underutilized and under Threat? BioScience. 2011;61(7):559-65.
11. Zhang X, Chen J, Liu X, Gao M, Chen X, Huang C. Nickel uptake and distribution in *Agropyron cristatum* L. in the presence of pyrene. Ecotoxicol Environ Saf. 2019;174:370-6.
12. Zhang J, Stevens PF, Zhang W. Evolution and development of inflorescences and floral symmetry in Solanaceae. American Journal of Botany. 2022;109(5):746-67.
13. Qin H, Yi X. Mast seeding is stronger in taller plants. Front Plant Sci. 2024;15:1382824.
14. Chen Y, Orlov YL, Chen M. Deciphering the Molecular Mechanism of the Intermediate Secondary Growth and Internode Elongation of the Castor Bean (Ricinus communis L.) by the Combined Analysis of the Transcriptome and Metabolome. International Journal of Molecular Sciences. 2024;25(2).
15. Kim DY, Hong MJ, Seo YW, McIntyre CL. Genome-wide transcript analysis of inflorescence development in wheat. Genome. 2019;62(9):623-33.
16. Zhao Y. Auxin biosynthesis and its role in plant development. Annu Rev Plant Biol. 2010;61:49-64.
17. Kasahara H. Current aspects of auxin biosynthesis in plants. Biosci Biotechnol Biochem. 2016;80(1):34-42.
18. Casanova-Saez R, Mateo-Bonmati E, Ljung K. Auxin Metabolism in Plants. Cold Spring Harb Perspect Biol. 2021;13(3).
19. Tivendale ND, Ross JJ, Cohen JD. The shifting paradigms of auxin biosynthesis. Trends Plant Sci. 2014;19(1):44-51.
20. Marzec M, Alqudah AM. Key Hormonal Components Regulate Agronomically Important Traits in Barley. Int J Mol Sci. 2018;19(3).
21. Youssef HM, Hansson M. Crosstalk among hormones in barley spike contributes to the yield. Plant Cell Rep. 2019;38(8):1013-6.
22. Serrano-Mislata A, Bencivenga S, Bush M, Schiessl K, Boden S, Sablowski R. DELLA genes restrict inflorescence meristem function independently of plant height. Nature Plants. 2017;3(9):749-54.
23. Li S, Zhao B, Yuan D, Duan M, Qian Q, Tang L, et al. Rice zinc finger protein DST enhances grain production through controlling
Gn1a/OsCKX2
expression. Proceedings of the National Academy of Sciences. 2013;110(8):3167-72.
24. Jameson PE, Song J. Cytokinin: a key driver of seed yield. J Exp Bot. 2016;67(3):593-606.
25. Bartrina I, Otto E, Strnad M, Werner T, Schmülling T. Cytokinin regulates the activity of reproductive meristems, flower organ size, ovule formation, and thus seed yield in Arabidopsis thaliana. Plant Cell. 2011;23(1):69-80.
26. Lang H, Zhang Y, Zhao S, Li K, Li X, Jiang M. Temporal Transcriptome Analysis Reveals Core Pathways and Orphan Gene EARLY FLOWERING 1 Regulating Floral Transition in Chinese Cabbage. Plants. 2025;14(14).
27. Weng X, Song H, Sreedasyam A, Haque T, Zhang L, Chen C, et al. Transcriptome and DNA methylome divergence of inflorescence development between 2 ecotypes in Panicum hallii. Plant Physiol. 2023;192(3):2374-93.
28. Davière JM, Achard P. Gibberellin signaling in plants. Development. 2013;140(6):1147-51.
29. Li S, Tian Y, Wu K, Ye Y, Yu J, Zhang J, et al. Modulating plant growth-metabolism coordination for sustainable agriculture. Nature. 2018;560(7720):595-600.
30. Yamaguchi N, Winter CM, Wu MF, Kanno Y, Yamaguchi A, Seo M, et al. Gibberellin acts positively then negatively to control onset of flower formation in Arabidopsis. Science. 2014;344(6184):638-41.

31. Pearce S, Vanzetti LS, Dubcovsky J. Exogenous gibberellins induce wheat spike development under short days only in the presence of VERNALIZATION1. Plant Physiol. 2013;163(3):1433-45.
32. Sakamoto T, Miura K, Itoh H, Tatsumi T, Ueguchi-Tanaka M, Ishiyama K, et al. An overview of gibberellin metabolism enzyme genes and their related mutants in rice. Plant Physiol. 2004;134(4):1642-53.
33. Benková E, Michniewicz M, Sauer M, Teichmann T, Seifertová D, Jürgens G, et al. Local, efflux-dependent auxin gradients as a common module for plant organ formation. Cell. 2003;115(5):591-602.
34. Gallavotti A. The role of auxin in shaping shoot architecture. J Exp Bot. 2013;64(9):2593-608.
35. Zhao Y, Christensen SK, Fankhauser C, Cashman JR, Cohen JD, Weigel D, et al. A role for flavin monooxygenase-like enzymes in auxin biosynthesis. Science. 2001;291(5502):306-9.
36. Kurakawa T, Ueda N, Maekawa M, Kobayashi K, Kojima M, Nagato Y, et al. Direct control of shoot meristem activity by a cytokinin-activating enzyme. Nature. 2007;445(7128):652-5.
37. Ashikari M, Sakakibara H, Lin S, Yamamoto T, Takashi T, Nishimura A, et al. Cytokinin oxidase regulates rice grain production. Science. 2005;309(5735):741-5.
38. Miyawaki K, Tarkowski P, Matsumoto-Kitano M, Kato T, Sato S, Tarkowska D, et al. Roles of Arabidopsis ATP/ADP isopentenyltransferases and tRNA isopentenyltransferases in cytokinin biosynthesis. Proc Natl Acad Sci U S A. 2006;103(44):16598-603.
39. Fleet CM, Sun TP. A DELLAcate balance: the role of gibberellin in plant morphogenesis. Curr Opin Plant Biol. 2005;8(1):77-85.
40. Reinhardt D, Pesce ER, Stieger P, Mandel T, Baltensperger K, Bennett M, et al. Regulation of phyllotaxis by polar auxin transport. Nature. 2003;426(6964):255-60.
41. Kieber JJ, Schaller GE. Cytokinin signaling in plant development. Development. 2018;145(4).
42. Shim Y, Lim C, Seong G, Choi Y, Kang K, Paek NC. The AP2/ERF transcription factor LATE FLOWERING SEMI-DWARF suppresses long-day-dependent repression of flowering. Plant Cell Environ. 2022;45(8):2446-59.
43. Song S, Qi T, Huang H, Ren Q, Wu D, Chang C, et al. The Jasmonate-ZIM domain proteins interact with the R2R3-MYB transcription factors MYB21 and MYB24 to affect Jasmonate-regulated stamen development in Arabidopsis. Plant Cell. 2011;23(3):1000-13.
44. Viola IL, Gonzalez DH. TCP Transcription Factors in Plant Reproductive Development: Juggling Multiple Roles. Biomolecules. 2023;13(5).
45. Lucero LE, Manavella PA, Gras DE, Ariel FD, Gonzalez DH. Class I and Class II TCP Transcription Factors Modulate SOC1-Dependent Flowering at Multiple Levels. Mol Plant. 2017;10(12):1571-4.
46. Li X, Zhang G, Liang Y, Hu L, Zhu B, Qi D, et al. TCP7 interacts with Nuclear Factor-Ys to promote flowering by directly regulating SOC1 in Arabidopsis. Plant J. 2021;108(5):1493-506.
47. Camoirano A, Alem AL, Gonzalez DH, Viola IL. The N-terminal region located upstream of the TCP domain is responsible for the antagonistic action of the Arabidopsis thaliana TCP8 and TCP23 transcription factors on flowering time. Plant Sci. 2023;328:111571.
48. Studer AJ, Wang H, Doebley JF. Selection During Maize Domestication Targeted a Gene Network Controlling Plant and Inflorescence Architecture. Genetics. 2017;207(2):755-65.
49. Thirulogachandar V, Govind G, Hensel G, Kale SM, Kuhlmann M, Eschen-Lippold L, et al. HOMEOBOX2, the paralog of SIX-ROWED SPIKE1/HOMEOBOX1, is dispensable for barley spikelet development. J Exp Bot. 2024;75(10):2900-16.
50. Riccucci E, Vanni C, Vangelisti A, Fambrini M, Giordani T, Cavallini A, et al. Genome-Wide Analysis of WOX Multigene Family in Sunflower (Helianthus annuus L.). Int J Mol Sci. 2023;24(4).
51. Himi S, Sano R, Nishiyama T, Tanahashi T, Kato M, Ueda K, et al. Evolution of MADS-box gene induction by FLO/LFY genes. J Mol Evol. 2001;53(4-5):387-93.
52. Huang X, Ma Z, He D, Han X, Liu X, Dong Q, et al. Molecular condensation of the CO/NF-YB/NF-YC/FT complex gates floral transition in Arabidopsis. Embo j. 2025;44(1):225-50.
53. Li Y, Zhou C, Yan X, Zhang J, Xu J. Simultaneous analysis of ten phytohormones in Sargassum horneri by high-performance liquid chromatography with electrospray ionization tandem mass spectrometry. J Sep Sci. 2016;39(10):1804-13.
54. Shannon, P.; Markiel, A.; Ozier, O.; Baliga, N.S.; Wang, J.T.; Ramage, D.; Amin, N.; Schwikowski, B.; Ideker, T. Cytoscape: A software environment for integrated models of biomolecular interaction networks. Genome Res. 2003, 13, 2498–2504.

Acknowledgements

We are deeply grateful to Professor Lei Liu for his invaluable guidance and insightful suggestions throughout the preparation of this manuscript. This research was funded by National Key Research and Development Program of China, grant number 2023YFD1200300.

Patents

Funding: “This research was funded by National Key Research and Development Program of China, grant number 2023YFD1200300”.

Data Availability

All data are open and available. The raw data are available in the NCBI database (BioProject ID PRJNA1390706) (https://www.ncbi.nlm.nih.gov/sra/PRJNA1390706) (accessed on 16 December 2025).

Author contributions statement

Conceptualization, X.Q. and Y.Y.; data curation, Y.Y.; writing—original draft preparation, Y.Y.; writing—review and editing, X.Q., F.H., Y.M., Z.L. and L.L. All authors have read and agreed to the published version of the manuscript.

Additional information

The authors declare no conflict of interest.

Supplementary Files

This is a list of supplementary files associated with this preprint. Click to download.

- SupplementaryMaterials.docx